



Seventh FRAMEWORK PROGRAMME THEME 6 Environment

Collaborative Project (Large-scale Integrating Project)

Project no. 212085

Project acronym: **MEECE**

Project title: Marine Ecosystem Evolution in a Changing Environment

D3.4 Synthesis report for Climate Simulations

Part 7: Adriatic Sea

Due date of deliverable: 30/08/2012

Actual submission date: 21/02/2013

Lead partner responsible for deliverable: AZTI-Tecnalia

Project co-funded by the European Commission within the Seventh Framework Programme, Theme 6 Environment		
Dissemination Level		
PU	Public	x
PP	Restricted to other programme participants (including the Commission)	
RE	Restricted to a group specified by the consortium (including the Commission)	
CO	Confidential, only for members of the consortium (including the Commission)	

Start date of project: 01.09.09 Duration: 54 months (including extension)

Project Coordinator: Icarus Allen, Plymouth Marine Laboratory

D3.4 Synthesis report for Climate Simulations

Part 7: Adriatic Sea

Contributors:

Marco Zavatarelli, Emanuela Clementi
UNIBO, Italy

Table of contents

1. Science questions	3
2. Models	3
3. Scenarios	3
4. Metrics considered and Validation	4
5. Linkages with MEECE deliverables	5
6. Results	5
6.1. Hindcast validation	5
6.2. Climate forced simulations	9
7. Discussion	10
8. Concluding remarks	13
9. References	14

1. Science questions

The enclosed Adriatic Sea is a very challenging basin for a modelling effort aimed to hindcast and predict (under scenario assumptions) its environmental dynamics. Its physical and biological oceanographic characteristics shift within a limited space range to truly coastal conditions (northern Adriatic Sea) to almost open ocean conditions (southern Adriatic Sea). The basin is known to have a large spatial and temporal variability (both seasonal and interannual) depending on its forcing drivers (atmospheric and land based). In addition, the basin is subject to a strong anthropogenic pressure. It is therefore important to assess both the extent of the changes in the Adriatic Sea as a function of both the climatic and the (direct) anthropogenic forcing.

2. Models

The full atmospheric dataset needed to formulate the surface open boundary condition for the model was obtained (for both the hindcast and the scenario simulations) from the output of the limited area ocean atmosphere model “EBU-POM” implemented over the Mediterranean Sea region. Details of the modelling system and of the data used to formulate the atmospheric forcing functions (surface fluxes of momentum, heat and mass) for the Adriatic Model are given in MEECE deliverable [D3.1](#) (“Common set of forcing scenarios”).

The coupled Physical LTL biogeochemical model implemented in the Adriatic Sea is the BFM-POM (Princeton Ocean Model - Biogeochemical Flux Model) modelling system. Details of the system are given in MEECE deliverable [D4.5](#) (*Summary of model systems, scenarios validation metrics and output for each region*).

The HTL model linked to the POM-BFM system is the OSMOSE model. Details of the system are given in the MEECE deliverable [D2.3](#) (“*Sub-model OSMOSE, Functional coupling with plankton models*”).

3. Scenarios

Even if MEECE WP3 deals particularly with climate issues, a hindcast (as well as a scenario prediction) of the Adriatic Sea environmental dynamics cannot ignore the role of the land based forcings (river runoff and nutrient load). The Adriatic Sea modelling effort could exploit the use of a high quality dataset to formulate the river runoff and the land based (riverborne) nutrient load. The dataset (Ludwig et al., 2005) originates from the EU-FP6 Project “SESAME” and provides the interannually varying (with a monthly resolution) Mediterranean river runoff and nutrient load for the both time slices considered by MEECE. These data were obtained by running a hydrological model (implemented over the Mediterranean Sea watershed) forced with

atmospheric data according to the MEECE time slices and consistent with the set of forcing functions used to force the Adriatic Model. Other parameters needed to define the nutrient load and the runoff were adopted consistently to current conditions for the hindcast time slice and adopting the “Business as usual (BaU)” assumption (extrapolation of current trends) for the scenario time slice.

The Adriatic Sea MEECE WP3 hindcast and scenario simulations (projections) encompass the following time slices:

- Hindcast: 1980-2010
- Scenario (projections): 2080-2100

The hindcast time slice was carried out utilising atmospheric forcing functions representing the current level of atmospheric CO₂, while scenario simulations are forced with the Global CO₂ emission scenario A1B.

4. Metrics considered and Validation

The model performance was validated by assessing the model results against the remotely-sensed (satellite observations) AVHRR SST (Sea Surface temperature), and against the remotely-sensed SeaWiFs surface pigments. The time slices available for the validation issues are:

- AVHRR (SST): 1985-2007
- SeaWifs (pigments): 1998-2010

The assessment of the model skill was carried out by adopting the objective validation methods detailed and described in MEECE [Deliverable D2.7](#) (“*user guide and report outlining validation methodology*”). The model results from the hindcast simulations were, therefore, assessed through Taylor diagrams, Target plots, as well as through the computation of the Model efficiency and reliability indexes.

The metrics considered were thus SST and surface chlorophyll concentration. Given the long time series available from the satellite observations, these two properties allow to carry out an appropriate validation of a long term simulations. Moreover, SST and chlorophyll are two central ocean properties computed by the physical and biogeochemical model, respectively, and allow us to test the model skill in addressing the following MSFD descriptors:

- 1.2.1 (phytoplankton) population biomass
- 5: Human induced eutrophication
- 7: Hydrographical conditions

5. Linkages with MEECE deliverables

The Adriatic Sea modelling effort benefitted from the output of the following MEECE deliverables.

Deliverable (see Table 3)	Comments
D2.3	LTL-HTL Link
D2.7	Model results validation
D3.2	Metric definitions

6. Results

6.1. Hindcast validation

Physical model

Fig. 1a show the SST Taylor diagram, the Target plot and the annual values of the Model efficiency and the model reliability indexes computed to obtain an objective assessment of the model simulation quality. The Taylor diagram (Fig. 1a) indicates that the model results are highly correlated with the observations and also show a good agreement between the observed and the modelled variability. The Target plots (fig. 1b) indicates that on the annual scale the model bias and the model RMSD (both normalised by the observation standard deviation) have a value lower than 1, which indicates that the model hindcasted fields are better descriptors than the average of the observations. The model efficiency (Nash-Sutcliffe, fig. 1c) index indicates, for each simulated year a value that allows the simulations to be defined as “excellent”. Finally the reliability index (multiplicative factor through which the model predict observation; see fig 1d), has a value ranging between 1.09 and 1.11. This indicates a certain disagreement between the model and the observations. The extent of the disagreement is shown in whole simulation period (1980-2010) in Fig. 2. For the period 1985-2007, the figure 2 reports also the remotely-sensed (AVHRR) SST time series compared with the model results. The model simulated SST has a seasonal cycle in agreement with the remote observations, although the hindcasted SST is clearly overestimated. Both the simulated and the observed time series indicate a long-term warming trend of the Adriatic sea SST.

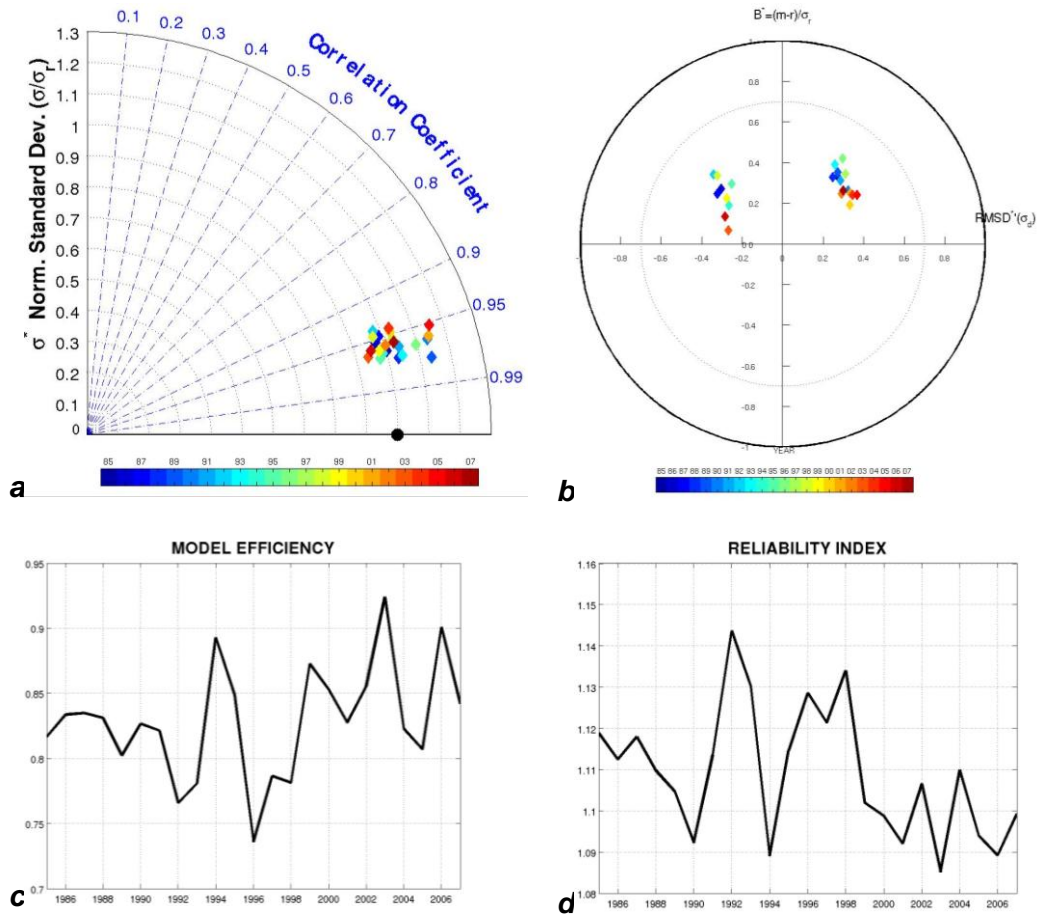


Figure 1. Sea Surface temperature: assessment of the model simulation quality against the 1985-2007 AVHRR observations. a. Taylor Diagram; b. Target plot; c. Model efficiency index. d. Model reliability index.

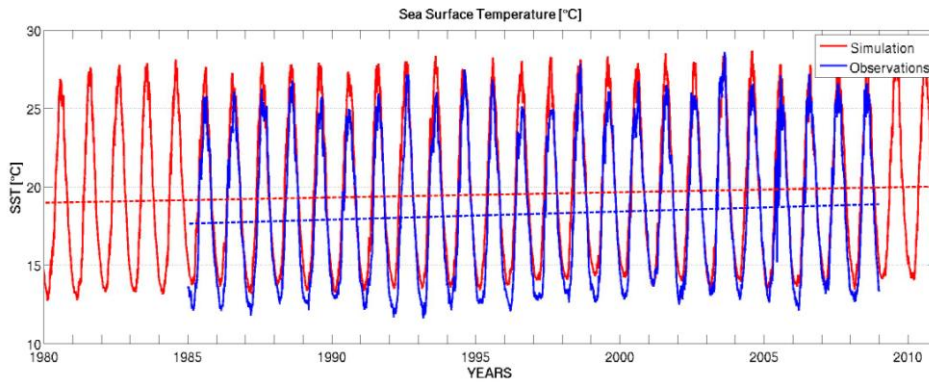


Figure 2. Sea surface temperature. Observed 1985-2007 (blue line) and simulated 1980-2010 (red line) SST time series. The dashed lines are the linear regression models computed for both time series.

The warming trend can be appreciated by the regression lines computed from both the observed and the simulated SST (fig. 2). Both trends (despite a tendency to a slower warming shown by the simulated SST) are in good agreement.

LTL model

Fig. 3 reports the Sea surface chlorophyll Taylor diagram, the Target plot and the annual values of the Model efficiency and the model reliability indexes computed to obtain an assessment of the model simulation quality. The Taylor diagram (Fig. 3a), report a correlation between hindcasted and simulated data ranging between 0.5 and 0.6 and a modelled variability basically lower than that characterising the observations.

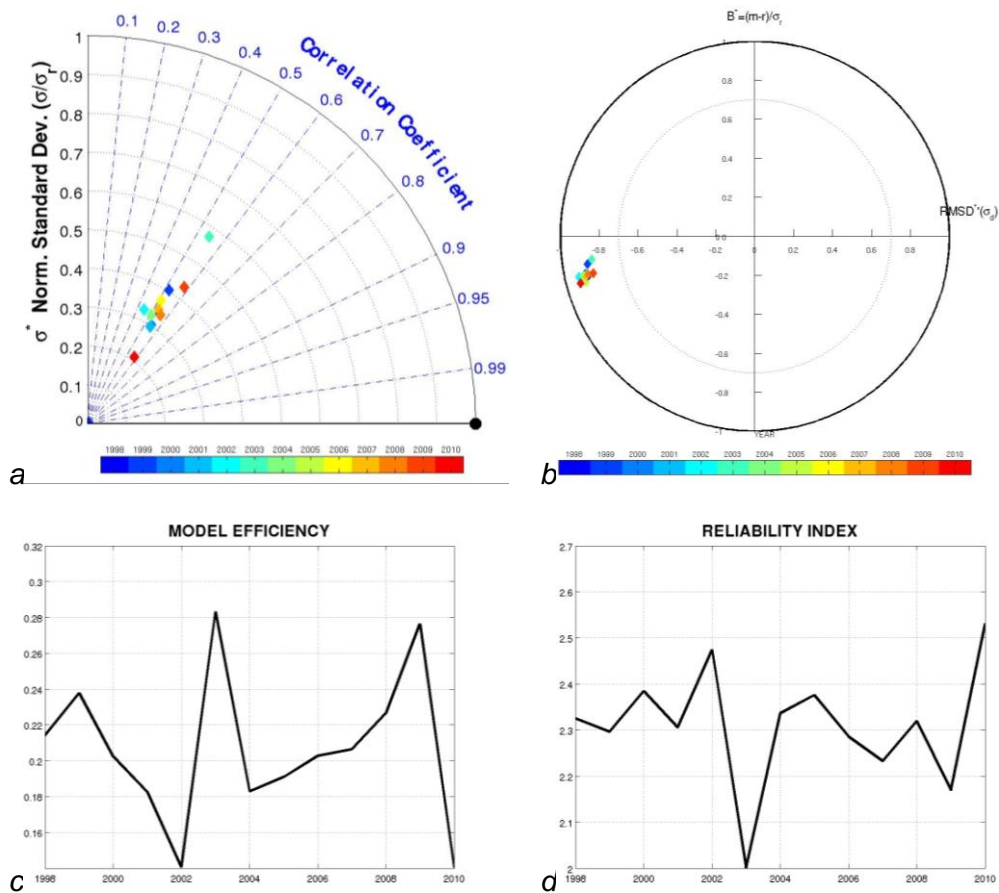


Figure 3. Sea Surface Chlorophyll: assessment of the model simulation quality against the 1998-2010 SeaWiFS surface pigments observations. a. Taylor Diagram; b. Target plot; c. Model efficiency index. d. Model reliability index.

The target plots (Fig. 3b) indicates that on the annual scale the model bias and the model RMSD (both normalised by the observation standard deviation) have a value of about 1.09-1.14, therefore indicating that the model hindcasted fields are better

descriptors than the average of the observations. However, the quality of the chlorophyll predictions is lower than the corresponding SST simulations. This is confirmed also by the model efficiency (Nash-Sutcliffe, fig. 3c) index that achieves lower values than those achieved by the SST validation. However, values above zero still indicate a certain model skill. Finally, the reliability index (multiplicative factor through which the model predict observation) of fig 3d, varying between 2.0 and 2.5, define the disagreement between the modelled and the observed values. This disagreement correspond to an overall model underestimation of the surface chlorophyll as depicted by Fig. 4 that shows the time series of the model simulated surface chlorophyll for the whole simulation period (1980-2010). For the period 1998-2010, the figure shows also the remotely-sensed (SeaWifs) surface pigments time series compared with the model results. It can be seen that both the observations and the hindcasted data identifies a long term decrease. However, Fig. 4 does not report a single regression line computed from the whole simulated time series. The progressive decrease of the simulated chlorophyll concentration from 1980 to 2010 does not occur with a continuous mode, but is characterised by two discontinuity points at the end of the 80's and at the end of the 90's. Thus, the regression lines have been computed separately for the last two decades of the 20th century and for the first decade of the 21st century. For the former decade, a good agreement between the simulated and the observed long-term trend exists.

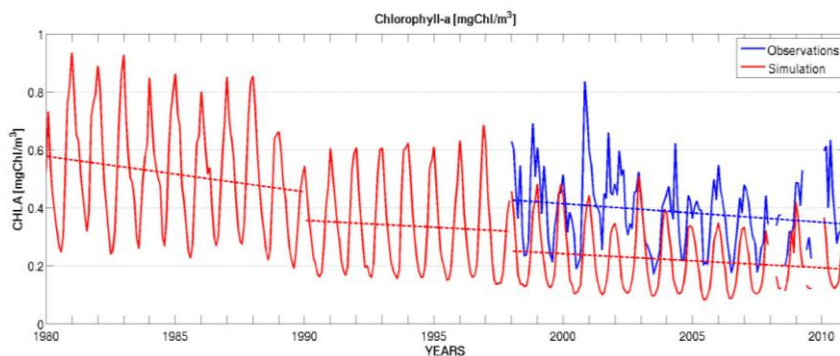


Figure 4. Sea surface chlorophyll. Observed 1998-2010 (blue line) and simulated 1980-2010 (red line) chlorophyll time series. The dashed lines are the regression lines computed from both time series.

A relatively good agreement between the simulated and the observed long-term trends can be observed also from the spatial distribution map of the trend computed at each model grid point (fig. 5).

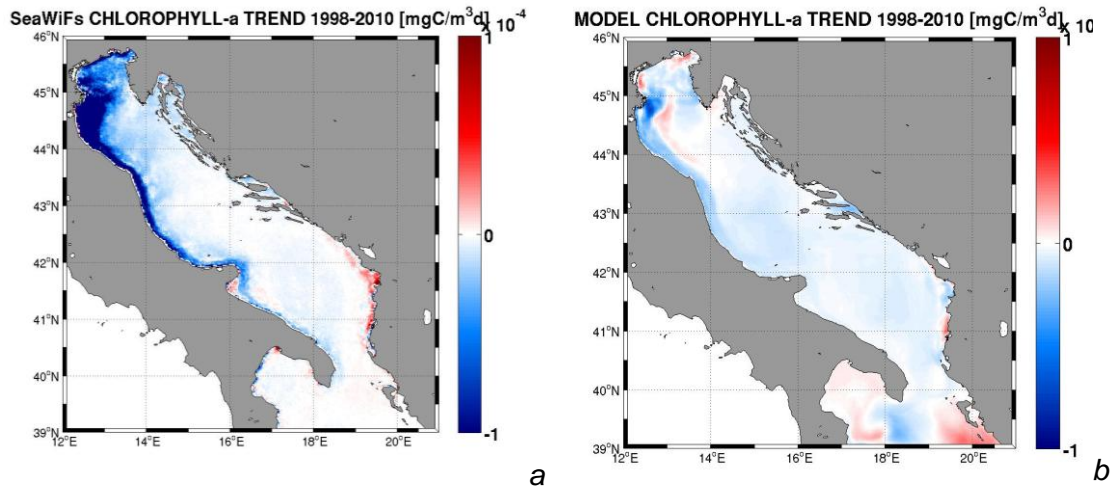


Figure 5. Sea surface chlorophyll trends. 1998-2010 Observed (a) and simulated (b) 1980-2010 spatial distribution of the chlorophyll temporal trend.

6.2. Climate forced simulations

Physical model

Fig 6. shows the time series of the simulated SST obtained for the time slice 2080-2100 under the A1b scenario. The warming trend described within the hindcasted time slice is evident also at the end of the 21st century and the long term trend is coherent with that defined by the hindcast simulations.

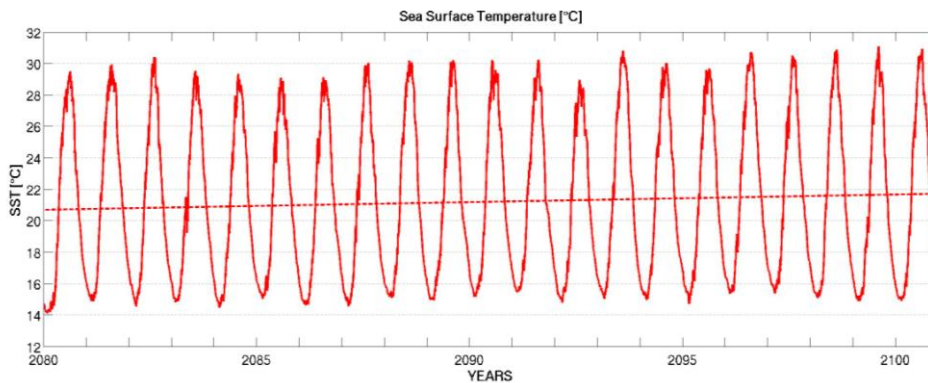


Figure 6. Sea surface temperature. Simulated 2080-2100 time series.

LTL model

Fig 7. show the time series of the simulated Sea Surface chlorophyll obtained for the time slice 2080-2100 under the A1b scenario. Also in the last two decades of the 21st century, the surface phytoplankton biomass decreases. However, the trend is slower than that estimated in the hindcast and in general the phytoplankton biomass seems

to approximately stabilise around the values occurring (in the hindcasted time slice) during the 2090s.

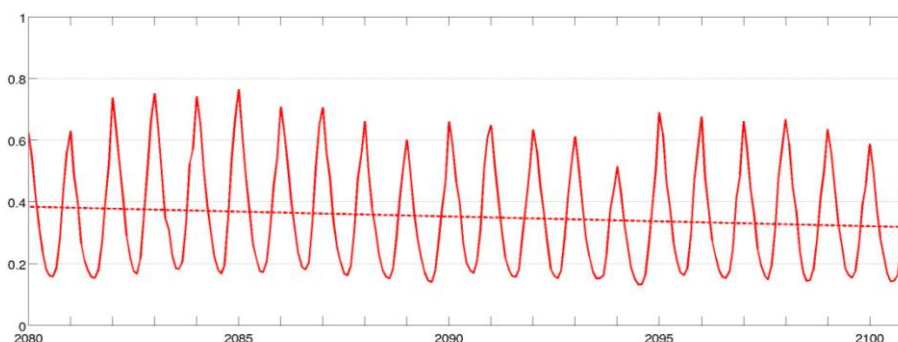


Figure 6. Sea surface Chlorophyll. Simulated 2080-2100 time series.

7. Discussion

What changes occur?

In this synthesis, the simulations of the Adriatic Sea coupled physical biogeochemical dynamics in hindcasted and scenario mode indicate two major changes: the progressive warming of the basin and the progressive decrease of the phytoplankton biomass. Such decreasing trend is rather apparent for the hindcasted period, while for the scenario simulation of the last two decades of the 21st century, the phytoplankton biomass stabilise around the values hindcasted for the 2090s (although with a weak decreasing trend).

Table 1 provides estimates of these changes in terms of absolute SST difference, and fractional changes of primary productivity, phytoplankton and zooplankton biomass. In the following sections, these trends are analysed in-depth with the help of the long-term annually averaged vertical profiles of temperature, phosphate, chlorophyll, and net primary productivity. The focus will be on the role of the climate in determining these change, although the use of high quality hindcast and scenario land-based forcing functions makes these simulations also very interesting for the relative assessment of the direct anthropogenic drivers impact (see WP4) on the Adriatic Sea Ecosystem dynamics, since the data used for providing the riverborne nutrient load account for the progressive decrease (from mid-80's onward) of the phosphate load in river water as a result of the policy measures undertaken to reduce the phosphorous load.

Table 1. Change of main climate changes and ecosystem response at 2080-2100 relative to 1980-2000 (Scenario A1B, Run3b: SINTEX-G forcing + future baseline river inputs + PISCES boundary condition for DIC/TA, see Table 1) in the N. Aegean Sea. Legend: For model uncertainty (based on hindcast validation), Low: the model describes interannual, seasonal and spatial variability appropriately, Medium: the model describes the general observed seasonal and spatial variability, High: the model fails in describing the general pattern (seasonal and spatial). For spatial variability, Low: most of areas with same trends, High: some areas with opposite trends with respect to others. Units: SST (°C), pH (surface), netPP: Net Primary Production Depth integrated, Zooplankton (biomass depth integrated). Range is expressed in Percentile 25 and Percentile 75. Absolute change for SST and pH. Fractional change for netPP, Zooplankton biomass and HTL; fractional change = $(A1B_{(2080-2100)}/PD_{(1980-2000)})-1$; see Holt et al. (2012); where -1 to 0: decrease, positive values: increase.

	Change range at 2080-2100 relative to 1980-2000				
	SST	pH	netPP	Phytoplankton biomass	Zooplankton biomass
Mean	1.75±0.11	N/A	0.162±0.026	-0.004 ^{ns} ±0.047	0.019 ^{ns} ±0.095
Range	+1.63; +1.79	N/A	+0.10; +0.18	N/A	-0.07; +0.04
Test kruskal-Wallis (p-value)	1.042e-14	N/A	2.016e-06	0.3543	0.06731
Model Uncertainty	Medium	N/A	High	High	High
Spatial variability	Low	N/A	High	High	High

Such sensitivity of the Adriatic Sea to land based nutrient input is discussed somehow in-depth in the WP4 deliverables.

How is climate driving these changes?

Keeping in mind that (as stated previously) the large changes in the Adriatic Sea ecosystem structure seems to be mainly driven by the land-based nutrient input, we summarise here the observed changes in the hydrological and biogeochemical structure, trying to define the role of the climate driver in modulating such changes.

Fig. 8 provides the annually averaged hindcasted and predicted vertical temperature profiles for the Northern, middle and southern Adriatic.

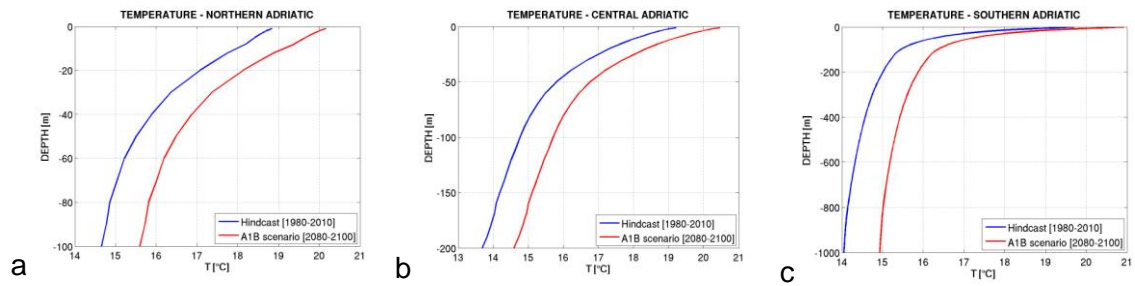


Figure 8. Annually averaged hindcasted (blue line) and predicted (red line) temperature (°C) vertical profiles for the northern (a), middle (b) and southern (c) Adriatic Sea.

The water column warming is significant in all the three subregions of the basin. The largest surface warming is observed in the northern and in the southern Adriatic. In the deeper part of the water column the model indicate an almost ubiquitous 1°C warming.

The warming correspond also, at least for the southern and middle Adriatic sea, to a stronger vertical stratification that might have concurred to the reduction of the surface phytoplankton biomass by limiting the nutrient supply from the deeper layers.

The progressive reduction of the phosphate load from rivers is reflected also on the state of the total phosphate pool simulated by the model. The annually averaged phosphate vertical profiles shown in Fig. 9 indicate a decrease of the deep nutrient pool of the middle and central Adriatic Sea by the end of the 21st century.

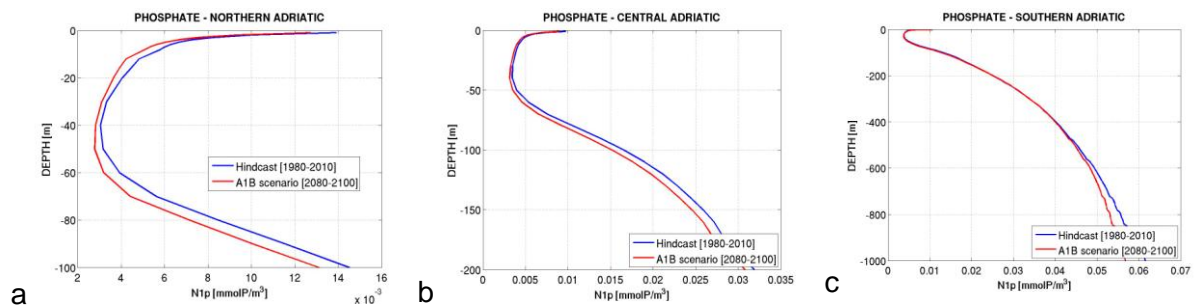


Figure 9. Annually averaged hindcasted (blue line) and predicted (red line) phosphate (mmol P/m³) vertical profiles for the northern (a), middle (b) and southern (c) Adriatic Sea.

The annually averaged chlorophyll profiles shown in Fig. 10 indicate how the reduction of the phosphate load from the river determine an overall decrease of the phytoplankton pool at all depths (not only at surface) and in all the basin subregions, indicating the shift of the Adriatic Sea towards more oligotrophic conditions.

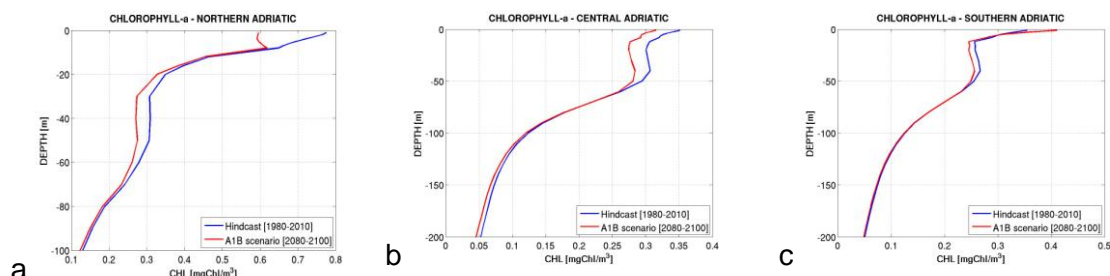


Figure 10. Annually averaged hindcasted (blue line) and predicted (red line) chlorophyll-a (mg/m^3) vertical profiles for the northern (a), middle (b) and southern (c) Adriatic Sea.

8. Concluding remarks

Main climate projections and ecosystem responses

- Oceanic warming and physical variables.** The simulations of the Adriatic Sea coupled physical biogeochemical dynamics in hindcasted and scenario models indicate the progressive warming of the basin ($+1.8^\circ\text{C}$). The water column warming is significant in all the three subregions of the basin. The largest surface warming is observed in the northern and in the southern Adriatic. In the deeper part of the water column the model indicate an almost ubiquitous 1°C warming.
- Lower trophic level.** An increase of net primary production (16%) is expected by the end of the century under climate change scenario, especially in the coastal zone. Mean phytoplankton and zooplankton biomass are not expected to change, whereas they will slightly increase in some coastal areas and decrease in offshore.

Impact to MSFD descriptors

- Human-induced eutrophication.** Climate change will slightly favour the risk of eutrophication at very particular coastal zones where primary production is expected to increase. However, anthropogenic scenarios (see WP4) indicate that reduction of the phosphate load from the river determine an overall decrease of the phytoplankton pool at all depths (not only at surface) and in all the basin subregions, indicating the shift of the Adriatic Sea towards more oligotrophic conditions. On the other hand, the lower trophic level dynamics of the basin are very sensitive to variation in the land-based nutrient load.

9. References

Ludwig, W., Dumont, E., Meybeck M., Heussner, S. (2005). River discharges of water and nutrients to the Mediterranean and Black Sea: Major drivers for ecosystem changes during past and future decades? *Progress in Oceanography*.

Ludwig, W., Bouwman, L., Dumont, E., Lepines, E. Water and nutrient fluxes from major Mediterranean and Black Sea rivers: past and future trends and their implication for the basin scale budgets. *Global biogeochemical cycles*.